BRL-MR-3759

(4)

MEMORANDUM REPORT BRL-MR-3759

BRL

AD-A208 105

ADIABATIC SH .\ BANDS IN ONE DIMENSION

T. W. WRIGHT
J. W. WALTER

MAY 1989

U.S. ARMY LABORATORY COMMAND

BALLISTIC RESEARCH LABORATORY
ABERDEEN PROVING GROUND, MARYLAND

DESTRUCTION NOTICE

Destroy this report when it is no longer needed. DO NOT return it to the originator.

Additional copies of this report may be obtained from the National Technical Information Service, U.S. Department of Commerce, Springfield, VA 22161.

The findings of this report are not to be construed as an official Department of the Army position, unless so designated by other authorized documents.

The use of trade names or manufacturers' names in this report does not constitute indorsement of any commercial product.

UNCLASSIFIED

SECURITY CLASSIFICATION OF THIS PAGE

REPORT DOCUMENTATION PAGE

Form Approved OMB No. 0704-0188

1a. REPORT SECURITY CLASSIFICATION Unclassified	1b. RESTRICTIVE MARKINGS
2a. SECURITY CLASSIFICATION AUTHORITY	3. DISTRIBUTION/AVAILABILITY OF REPORT APPROVED FOR PUBLIC RELEASE; DISTRIBUTION UNLIMITED.
2b. DECLASSIFICATION/DOWNGRADING SCHEDULE	
4. PERFORMING ORGANIZATION REPORT NUMBER(S) BRL-MR-3759	5. MONITORING ORGANIZATION REPORT NUMBER(S)
6a. NAME OF PERFORMING ORGANIZATION Ballistic Research Laboratory 6b. OFFICE SYMBOL (If applicable) SLCBR-TB	7a. NAME OF MONITORING ORGANIZATION
6c. ADDRESS (City, State, and ZIP Code) Aberdeen Proving Ground, MD 21005-5066	7b. ADDRESS (City, State, and ZIP Code)
8a. NAME OF FUNDING/SPONSORING ORGANIZATION 8b. OFFICE SYMBOL (If applicable)	9. PROCUREMENT INSTRUMENT IDENTIFICATION NUMBER
8c. ADDRESS (City, State, and ZIP Code)	10. SOURCE OF FUNDING NUMBERS PROGRAM ELEMENT NO. | PROJECT NO. | TASK NO. | WORK UNIT ACCESSION NO.

11. TITLE (Include Security Classification)

ADIABATIC SHEAR BANDS IN ONE DIMENSION

12. PERSONAL AUTHOR(S)

WRIGHT, Thomas W., WALTER John W.

13a. TYPE OF REPORT	13b. TIME COVERED	14. DATE OF REPORT (Year, Month, Day)	15. PAGE COUNT
BRL MR	FROM ______ TO ______		

16. SUPPLEMENTARY NOTATION

17. COSATI CODES		
FIELD	GROUP	SUB-GROUP
11	06	
20	11	

18. SUBJECT TERMS (Continue on reverse if necessary and identify by block number)

adiabatic shear ,

19. ABSTRACT (Continue on reverse if necessary and identify by block number)

This report summarizes the progress made at the Ballistic Research Laboratory to date in analyzing and understanding the dynamical processes that cause the formation of adiabatic shear bands and the influence of various physical parameters on their formation.

20. DISTRIBUTION/AVAILABILITY OF ABSTRACT ☒ UNCLASSIFIED/UNLIMITED ☐ SAME AS RPT. ☐ DTIC USERS	21. ABSTRACT SECURITY CLASSIFICATION Unclassified
22a. NAME OF RESPONSIBLE INDIVIDUAL John W. Walter	22b. TELEPHONE (Include Area Code) 301/278-6051 22c. OFFICE SYMBOL SLCBR-TB-W

DD Form 1473, JUN 86 Previous editions are obsolete.

SECURITY CLASSIFICATION OF THIS PAGE

UNCLASSIFIED

Contents

List of Figures

1 EQUATIONS OF MOTION

A simple one dimensional model, which may be thought of as simulating a torsional Kolsky bar test on a thin walled tube, has been studied extensively by both numerical and analytic techniques. For a body in simple shear

$$x = X + u(Y,t)\,, \qquad y = Y\,, \qquad z = Z\,, \tag{1}$$

the nondimensional equations of thermoviscoplasticity may be written as

$$\begin{array}{lrcl} \text{Momentum:} & v_t & = & s_y/\rho\,, \\ \text{Energy:} & \theta_t & = & k\theta_{yy} + s\dot{\gamma}_p\,, \\ \text{Elasticity:} & s_t & = & \mu(v_y - \dot{\gamma}_p)\,, \\ \text{Flow Law:} & s & = & \operatorname{sgn}(\dot{\gamma}_p)\kappa g(\theta)|\dot{\gamma}_p|^m\,, \\ \text{Work hardening:} & \kappa_t & = & M(\kappa,\theta)s\dot{\gamma}_p\,. \end{array} \tag{2}$$

where v is the velocity, θ is the temperature, s is the shear stress, κ is the work hardening parameter, $\dot{\gamma}_p$ is the plastic strain rate, and sgn indicates the algebraic sign of its argument.

Nondimensionalization follows the same scheme as used by [1], except that a dynamic value $s_0 = \kappa_0(b\dot{\gamma}_0)^m$ is used for the characteristic stress rather than the static value κ_0. Here $\dot{\gamma}_0$ is the imposed nominal strain rate (the velocity difference across the slab divided by the thickness) and κ_0 is the initial yield strength. The flow stress has been chosen to depend multiplicatively on functions of the temperature, the plastic strain rate, and a work hardening parameter, so that at its most general the material model includes work hardening and rate hardening, opposed by thermal softening. This combination, as is well known, can lead to strain softening, which in turn offers the opportunity for localization. Elasticity, inertia, and heat conduction all modulate the response in ways that are becoming increasingly clear. Of these three modulating effects, heat conduction appears to be the most important in that it is thermal conductivity that regularizes the governing equations and that ultimately limits the intensity of the localization and prevents formation of a singularity. No explicit failure criterion has been included in the model.

Only insulated boundaries with constant prescribed velocity are considered. That is, $\theta_y(\pm 1,t) = 0$ and $v(\pm 1,t) = \pm 1$. The initial strain rate is assumed to be close to unity everywhere, and the initial stress is assumed to be constant. To trigger a shear band, only perturbations in the initial temperature will be considered, $\theta(y,0) = \theta_0(y)$, where θ_0 is small. Mechanical perturbations can also initiate a shear band, but for brevity we will omit them here; see [2].

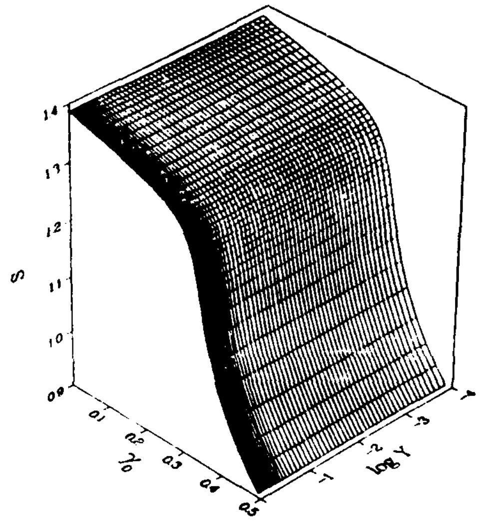

Figure 1: Stress response for a relatively low applied nominal strain rate, $\dot{\gamma}_0 = 50/s$.

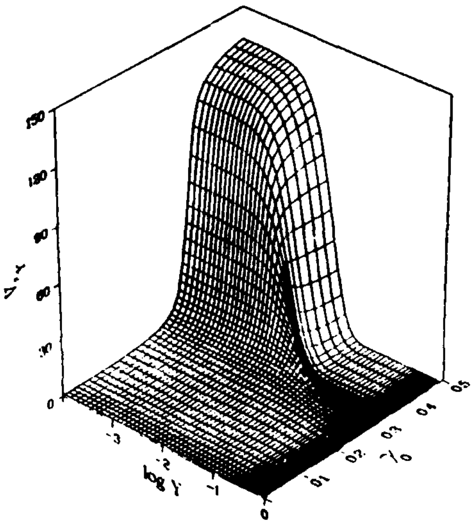

Figure 2: Velocity gradient for the same nominal strain rate.

2 FINITE ELEMENT SOLUTIONS

Finite element calculations, [3] and [4] are able to follow the development of the band through successive stages of formation, including early unstable growth, followed somewhat later by rapid localization and loss of stress carrying capacity, and culminating in a highly localized, late stage morphology. In the earlier calculations elasticity and work hardening were ignored, and linear thermal softening was assumed; the material parameters used were for a moderately high strength steel. Typical results from these calculations are shown in Figures 1 and 2. Note the slowly varying (post localization) late stage which is completely independent of the details of the initial conditions. Instead, it is determined solely by the functional form of the flow law, the various nondimensional parameters, the boundary conditions, and the applied nominal strain rate, $\dot{\gamma}_0$, with larger values of the latter corresponding to more intense localization.

These calculations, which treat the spatially discretized equations as a system of stiff ordinary differential equations for the temporal evolution of

the nodal values of v, θ, s, ψ, appear to be highly robust and to resolve the spatial and temporal features of the solution with complete fidelity. In many instances it is possible to exceed the Courant condition (based on the elastic wave speed) by several orders of magnitude so that, even though the required grid refinement may be on the order of 1/10000 of the spatial range or less, the computational time is often only a few minutes.

3 APPROXIMATE SOLUTIONS

Mathematical analysis yields several types of specialized solutions that illuminate the various regions of the overall numerical solution. Homogeneous solutions that vary in time, but not in space, reveal whether or not strain softening occurs for the particular constitutive equation in use. While these solutions usually can not be written down explicitly, the system of partial differential equations degenerates to a low order system of ordinary differential equations which can be solved numerically. For example, with $\theta_{yy} = 0$, (2.2) and (2.5) may be combined to give an ODE with solution $\kappa = \hat{\kappa}(\theta)$, and then (2.4) may be written $\dot{\gamma}_p = F(s, \theta)$. Finally, with $v_y = 1$, (2.2) and (2.3) may be combined and reduced to the ODE

$$\frac{1}{\mu}\frac{ds}{d\theta} = \frac{1 - F(s,\theta)}{sF(s,\theta)}, \qquad \text{with } s(0) = 1\,. \tag{3}$$

Inspection of this reduced system reveals that since the nondimensional elastic modulus $\mu = \bar{\mu}/s_0$ is generally rather large (in the range of 50 to 100) elasticity contributes only a boundary layer that modulates the stress as it decays to a characteristic function of temperature only, $F(s, \theta) = 1$, or reverting to (2.4), $s = \hat{\kappa}(\theta)g(\theta)$. This represents essentially rigid-plastic response. In inhomogeneous problems elasticity plays the same minor role up to the time of intense localization, and so will be ignored for the time being. Moreover, since the stress remains essentially constant in y prior to localization except at very high applied strain rates (e.g., $\dot{\gamma}_p > 10^4/s$, in the cases discussed here) it is sufficient to consider the quasi-static approximation in order to estimate the time to intense localization. Thus, for analytical purposes equations (2) may be replaced by the following simpler set

$$\begin{aligned} s_y &= 0\,, \\ \theta_t &= k\theta_{yy} + sv_y\,, \\ s &= \operatorname{sgn}(v_y)\kappa g(\theta)|v_y|^m\,, \\ \kappa_t &= M(\kappa, \theta)sv_y\,. \end{aligned} \tag{4}$$

Small perturbations about the homogeneous solution yield a system of linear partial differential equations, which may be inspected for stability of the underlying homogeneous solution. The difficulty here is that the perturbation equations have time varying coefficients since the underlying motion is unsteady. An explicit solution does not seem possible in general, but for the special case of a rigid-perfectly plastic material with power law rate hardening and linear thermal softening, an exact solution may be written down for a temperature perturbation, see Wright and Walter (1987). For example, the strain rate is given by

$$v_y = 1 + (\epsilon a/m)\exp(at/m)(\psi - 1), \tag{5}$$

where $\psi_t = k\psi_{yy}$, $\psi_y = 0$ at the boundaries, $\epsilon\psi_0 = \theta_0$ with $\int_0^1 \psi_0 \, dy = 1$, and the subscript 0 denotes initial conditions.

From such a solution a criterion for absolute stability of the homogeneous solution can be obtained, as well as the early growth rates for the field variables. Clearly, stability depends on the competition between the exponential factor and the diffusion factor. By inspection of (5) with ψ expressed by its Fourier components, it may be seen that for this solution to decay in time, a certain combination of material parameters, which we will call the "shear band susceptibility", must be less than the nondimensional thermal conductivity times π squared, $\chi_{SB} \equiv a/m < k\pi^2$. In dimensional terms this is

$$\chi_{SB} \equiv \frac{\bar{a}\kappa_0(b\dot{\gamma}_0)^m}{\rho c m} < \frac{k\pi^2}{\rho c\dot{\gamma}_0 H^2}, \tag{6}$$

where $\bar{a}$ is the negative of the initial slope of $g(\theta)$, κ_0 is the strength parameter, $\dot{\gamma}_0$ is the nominal strain rate, H is the half thickness in the slab, c is the heat capacity, and b is the characteristic time of the viscoplastic response.

If the homogeneous solution is not initially stable, then it is essentially the susceptibility that determines the initial growth rate. Of course, the long time behavior of the linearized system is meaningless when the underlying homogeneous flow is not stable. At present the perturbation equations that occur in the more general cases with work hardening can only be treated by special approximate techniques, but a different perturbation technique yields further insights when work hardening is absent.

By transforming variables, it is possible to find an approximate solution that for many cases appears to track the full finite element solution with great accuracy until immediately before intense localization occurs. Full details will be given by [2] but a sketch of the method as applied to a rigid-perfectly plastic material follows. Let $H(\theta) = \int_0^\theta g^{1/m} \, d\theta$ and let a new time scale $T(t)$ be defined by $dT/dt = s^{(1+m)/m}$. Now the energy equation may be

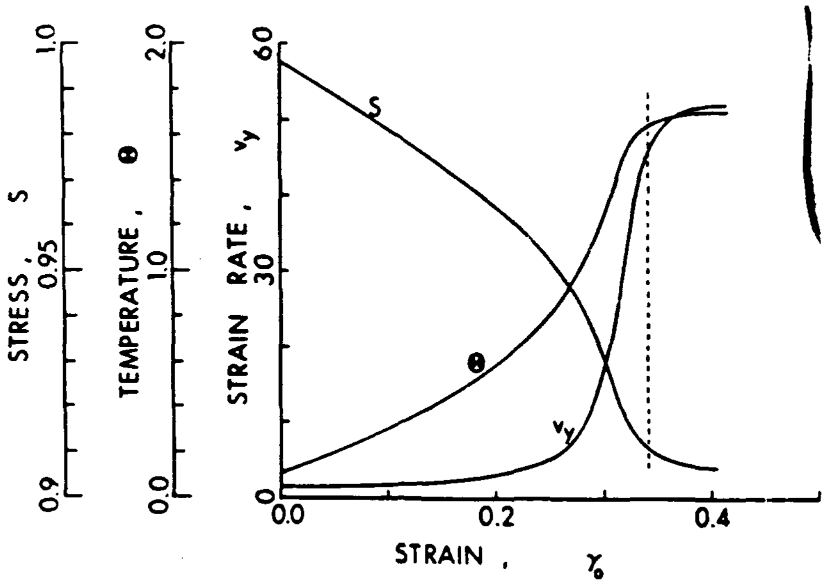

Figure 3: Shear band response by parametric solution for a typical case.

written as

$$H_T = 1 + k\frac{dt}{dT}(H_{yy} - \frac{H_{\theta\theta}}{H_\theta^2}H_y^2)\,. \tag{7}$$

Upon dropping the last term on the right hand side, an approximate solution may be obtained in the form

$$H = T + \psi\,, \quad s^{-1/m} = \int_0^1 g^{-1/m}\,dy\,, \quad dt/dT = s^{-(1+m)/m}\,, \tag{8}$$

in which $\psi_t = k\psi_{yy}$ and $\psi_0 = H(\theta_0)$. Equation (8.1) gives an implicit relationship among θ, t, T and y; equation (8.2) gives s as a function of both time scales and follows from use of (4.3) in the relation $\int_0^1 v_y\,dy = 1$; (8.3) is an ODE from which the dependence on t may be recovered.

This solution compares extremely well with the full finite element solution until the time of intense localization, [2], and is far easier to compute. Figure 3 shows the stress, temperature and strain rate in the center of the band as calculated from (8) for the same initial perturbation as used by [3]. Furthermore, from consideration of the simple defect structure $\theta_0(y) = \epsilon\cos\pi y$, it can easily be shown from (8) that the same shear band susceptibility mentioned previously is the most important physical quantity in determining the time or nominal strain from instability to intense local-

ization, [2]. The critical strain, γ_{cr}, in this case obeys the inequality

$$\gamma_{cr} \geq \frac{1}{\chi_{SB}} \ln \frac{2}{\epsilon \chi_{SB}} . \tag{9}$$

Heat conduction, which is primarily responsible for the inequality in (9), can have a substantial delaying effect on localization, especially at lower nominal strain rates. In fact, it is probably more accurate to say that localization occurs at a critical temperature, rather than at a critical strain. Heat conduction delays localization by reducing the temperature in the center of the band at a given nominal strain and spreading the thermal energy to the surrounding cooler material.

At higher rates inertial effects, which are not included in the parametric solution outlined here, become important and can also have a delaying effect on localization, [3]. A simple analysis and explanation for this effect is not yet available.

From the definition of H, expanded by use of Laplace's method, it also can be shown that to within a simple linear scaling, all rigid-perfectly plastic materials with fairly general thermal softening are equivalent to one that softens exponentially with temperature, [2], at least with respect to the critical localization strain for small perturbations. When there is only a temperature perturbation, it turns out that the critical strain may be estimated by solving (8.3), which now reads

$$\frac{dt}{d\hat{T}} = \frac{mC}{a} \left[\int_0^1 \frac{dy}{1-\hat{H}} \right]^{1+m} , \tag{10}$$

where $\hat{H} = 1 - g^{1/m} = \hat{T} + \psi(y,t)$ and ψ satisfies a diffusion equation as in (8). The constant $C = 1 + O(m)$ may be calculated from knowledge of the actual softening function. For softening functions with the same initial slope $-a$, C is exactly 1 for exponential softening, less than 1 for more rapid softening, and greater than 1 for weaker softening, but in no case does it depend on the softening behavior at large temperatures. This correspondence makes it vividly clear that the critical strain to localization for small perturbations is dominated by the thermal softening behavior near ambient temperature, and *not* by the behavior at large temperatures. In addition, more extensive finite element computations, to be reported by [4], indicate that the terms associated with C in the solution of (10) provide a correction of the proper sign and magnitude to the value of γ_{cr} as given by (9).

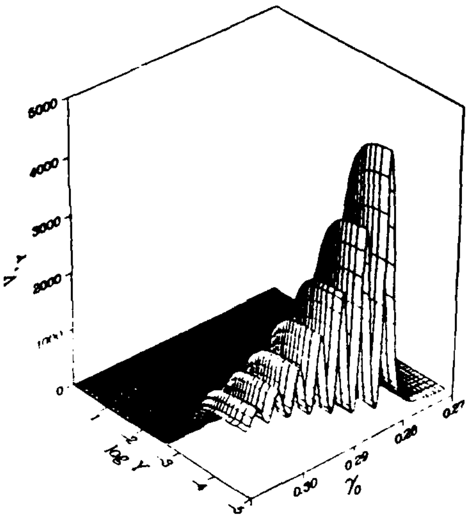

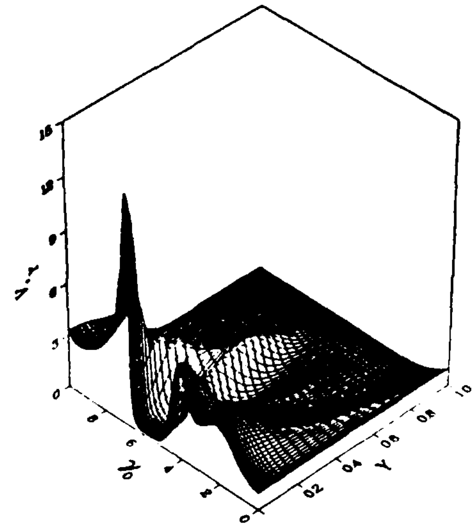

Figure 4: Velocity gradient for elastic perfectly-plastic case with $\dot{\gamma}_0 = 750/\mathrm{s}$.

Figure 5: Velocity gradient for full material model (copper data) at $\dot{\gamma}_0 = 330/\mathrm{s}$.

4 POST LOCALIZATION BEHAVIOR

In contrast to the results above, the late stage behavior within a shear band, after intense localization has occurred, must depend on high temperature response, but even then extreme temperatures do not necessarily occur. In the rigid-perfectly plastic case or if the work hardening saturates, the late stage morphology appears to be well represented by a rapidly shearing boundary layer in the center of the band and an exterior region where there is little or no further plastic work, and where temperature changes occur mainly by heat conduction from the actively shearing region. The solution in the core of the band is well represented by a steady solution, [2], which can be found from a simple quadrature, [5].

When work hardening and/or elasticity are restored, the full model is required once again. Numerical studies of (2) show that the localization and late stage response may become much more complex. Two notable effects will be reported in detail by [4] and are noted briefly here.

First of all with elasticity (but not work hardening) included, there can

be a considerable amount of elastic energy stored in the material outside the location at which the shear band will form. When intense localization occurs, this stored energy is released as the stress collapses in the band. In a narrow slab communication with the boundaries is rapid, and the net result is that the strain rate and velocity initially overshoot the values they would have attained in the rigid case followed by rapidly decaying oscillations, in which the stress and temperature also participate, before settling on the final late stage morphology as in Figure 4. The period of oscillation is longer (by a factor of about 10 in cases run to date) than that for an elastic wave communicating with the boundary, so these waves are clearly *not* simple damped elastic waves. Rather, they appear to be a consequence of the competing hardening and softening effects included in the model although they are, of course, elastically *driven* in the sense just outlined. The intensity of the overshoot and the severity of the oscillations seem to increase rapidly with increasing nominal strain rate. Both the initial overshoot and the oscillations are suppressed by an artificially high elastic modulus presumably because then there is less stored energy for a given stress level. Indeed, the (effectively) rigid cases illustated in the first two figures were obtained by using a value for μ equal to 100 times the physical value.

On the other hand, if work hardening continues throughout band formation, there may be repeated localizations on the same band whether or not elasticity is included. The first localization appears in the center of the original perturbation, but as the strain rate shoots up, so does the local rate of hardening. As κ increases the effect of thermal softening is overcome, and the strain rate at the slab center falls so that the peak rate occurs slightly to the sides. When these secondary peaks have experienced enough hardening in turn, the maximum strain rate returns to the center. Then the whole process can repeat as in Figure 5 where the material parameters used were for annealled copper. This gives the stress response a choppy, or irregularly oscillating appearance after the first localization, and can delay complete stress collapse to strains much larger than that at which the first localization occurs. It is also of interest to observe the very different time and length scales on which the localization occurs in Figure 4 and 5. The material model is the same in the two cases; only the parameter values are different.

5 SUMMARY

From a variety of analytical techniques it has been found that shear band formation is a multistep process, that instability and intense localization are not coincident in time, that a fully formed shear band often behaves like a boundary layer with a well defined, calculable, spatial distribution, and that a

theoretical "shear band susceptibility" can be identified and calculated from macroscopic laboratory measurements. The susceptibility, which appears naturally in simplified analyses, appears to be the key quantity in assessing stability, early growth rate, and time to intense localization. Elasticity has little effect until intense localization occurs, and then it may add rather elaborate structure to the late stage morphology. Work hardening, which is known to be stabilizing before localization, has a partially stabilizing effect after localization where it also adds structure to the late stage morphology.

References

[1] T. W. Wright and R. C. Batra. The interaction and growth of adiabatic shear bands. *Internat. J. Plast.*, 1:205–212, 1985.

[2] T. W. Wright. Approximate analysis for the formation of adiabatic shear bands. Submitted to *J. Mech. Phys. Solids*, Jan. 1989.

[3] T. W. Wright and J. W. Walter, Jr. On stress collapse in adiabatic shear bands. *J. Mech. Phys. Solids*, 35(6):701–720, 1987.

[4] J. W. Walter, Jr. Numerical experiments in adiabatic shear bands. In preparation, 1989.

[5] T. W. Wright. Steady shearing in a viscoplastic solid. *J. Mech. Phys. Solids*, 35(3):269–282, 1987.

DISTRIBUTION LIST

No. Copies	Organization
12	Administrator Defense Technical Information Center ATTN: DTIC-DDA Cameron Station Alexandria, VA 22304-6145
1	HQDA (SARD-TR) Washington, DC 20310-0001
1	Commander US Army Materiel Command ATTN: AMCDRA-ST 5001 Eisenhower Avenue Alexandria, VA 22333-0001
1	Commander US Army Laboratory Command ATTN: AMSLC-DL 2800 Powder Mill Road Adelphi, MD 20783-1145
1	Commander Armament RD&E Center US Army AMCCOM ATTN: SMCAR-MSI Picatinny Arsenal, NJ 07806-5000

No. Copies	Organization
1	Commander Armament RD&E Center US Army AMCCOM ATTN: SMCAR-TDC Picatinny Arsenal, NJ 07806-5000
1	Director Benet Weapons Laboratory Armament RD&E Center ATTN: SMCAR-LCB-TL Watervliet, NY 12189-4050
1	Commander US Army Armament, Munitions and Chemical Command ATTN: SMCAR-ESP-L Rock Island, IL 61299-5000
1	Commander US Army Aviation Systems Command ATTN: AMSAV-DACL 4300 Goodfellow Blvd. St Louis, MO 63120-1798
1	Director US Army Aviation Research and Technology Activity Ames Research Center Moffett Field, CA 94035-1099

DISTRIBUTION LIST

No. Copies	*Organization*
1	Commander US Army Missile Command ATTN: AMSMI-AS Redstone Arsenal, AL 35898-5010
1	Commander US Army Tank Automotive Command ATTN: AMSTA-TSL Warren, MI 48397-5000
1	Director US Army TRADOC Analysis Command ATTN: ATAA-SL White Sands Missle Range, NM 88002-5502
1	Commandant US Army Infantry School ATTN: ATSH-CD-CSO-OR Fort Benning, GA 31905-5660
1	AFWL/SUL Kirtland AFB, NM 87117-5800

No. Copies	*Organization*
1	Air Force Armament Labortory ATTN: AFATL/DLODL Eglin AFB, FL 32542-5000
	Army
3	Director US Army Research Office ATTN: J. Chandra I. Ahmad J. Wu PO Box 12211 Research Triangle Park, NC 27709-2211
3	Director US Army BMD Advanced Technology Center ATTN: ATC-T/M. Capps ATC-RN/P. Boyd ATC-M/S. Brockway ATTN: CRDABH-5/W. Loomis PO Box 1500, West Station Huntsville, AL 35807
1	Commander US Army Natick Research and Development Center ATTN: DRXRE/D. Sieling Natick, MA 01762

DISTRIBUTION LIST

No. Copies	Organization
3	Director US Army Materials Technology Laboratory ATTN: SLCMT-MRD/ J. Mescall S. Chou J. Dandekar Watertown, MA 021720-0001
2	Commander US Army RD&E Center ATTN: SMCAR-SC/ J. Corrie J. Beetle Dover, NJ 07801
1	Commander US Army Harry Diamond Laboratory ATTN: SLCHD-TA-L 2800 Powder Mill Road Adelphi, MD 20783

No. Copies	Organization
2	Office of Naval Research Dept. of the Navy ATTN: Y. Rajapakse A. Tucker Washington, DC 20360
1	Commander US Naval Air Systems Command ATTN: AIR-604 Washington, DC 20360
1	Commander Naval Sea Systems Command ATTN: Code SEA-62D Dept. of the Navy Washington, DC 20362-5101
3	Commander Naval Surface Weapons Center ATTN: W. Holt W. Mock Tech. Lib. Dahlgren, VA 22448-5000
3	Commander Naval Surface Weapons Center ATTN: R. Crowe Code R32/S. Fishman Code X211/Lib Silver Spring, MD 20902-5000

DISTRIBUTION LIST

No. Copies	Organization
1	US Naval Academy Dept. of Mathematics ATTN: R. Malek-Madani Annapolis, MD 21402
4	Air Force Armament Laboratory ATTN: J. Foster J. Collins J. Smith G. Spitale Eglin AFB, FL 32542-5438
1	Air Force Wright Aeronautical Laboratories Air Force Systems Command Materials Laboratory ATTN: T. Nicholas Wright-Patterson AFB, OH 45433
1	Air Force Wright Aeronautical Laboratories Air Force Systems Command Materials Laboratory ATTN: J. Henderson Wright-Patterson AFB, OH 45433
2	Director Defense Advanced Research Projects Agency ATTN: Tech Info B. Wilcox 1400 Wilson Blvd. Arlington, VA 22209
7	Sandia National Laboratories ATTN: L. Davison P. Chen W. Herrman J. Nunziato S. Passman E. Dunn M. Forrestal PO Box 5800 Albuquerque, NM 87185-5800
1	Sandia National Laboratories ATTN: D. Bammann Livermore, CA 94550
1	Director National Aeronautics and Space Administration Lyndon B. Johnson Space Center ATTN: Lib. Houston, TX 77058

DISTRIBUTION LIST

No. Copies	*Organization*
1	Director Jet Propulsion Laboratory ATTN: Lib. (TDS) 4800 Oak Grove Drive Pasadena, CA 91103
1	National Institute of Science and Technology ATTN: T. Burns Technology Building, Rm A151 Gaithersburg, MD 20899
	Universities
1	Forestal Research Center Aeronautical Engineering Laboratory Princeton University ATTN: A. Eringen Princeton, NJ 08540
1	University of Missouri-Rolla Dept. of Mechanical and Aerospace Engineering ATTN: R. Batra Rolla, MO 65401-0249
1	California Institute of Technology Division of Engineering and Applied Science ATTN: J. Knowles Pasadena, CA 91102

No. Copies	*Organization*
1	Denver Research Institute University of Denver ATTN: R. Recht PO Box 10127 Denver, CO 80210
1	Massachusetts Institute of Technology Dept. of Mechanical Engineering ATTN: L. Anand Cambridge, MA 02139
2	Rennselaer Polytechnic Institute Dept. of Mechanical Engineering ATTN: E. Lee E. Krempl Troy, NY 12181
1	Rennselaer Polytechnic Institute Dept. of Computer Science ATTN: J. Flaherty Troy, NY 12181
5	Brown University Division of Engineering ATTN: R. Clifton J. Duffy B. Freund A. Needleman R. Asaro Providence, RI 02912
1	Brown University Division of Applied Mathematics ATTN: C. Dafermos Providence, RI 02912

No. Copies	Organization
2	Carnegie-Mellon University Dept. of Mathematics ATTN: D. Owen M. Gurtin Pittsburg, PA 15213
6	Cornell University Dept. of Theoretical and Applied Mechanics ATTN: Y. Pao J. Jenkins P. Rosakis W. Sachse T. Healey A. Zehnder Ithaca, NY 14850
2	Harvard University Division of Engineering and Applied Physics ATTN: J. Rice J. Hutchinson Cambridge, MA 02138
2	Iowa State University Engineering Research Laboratory ATTN: A. Sedov G. Nariboli Ames, IA 50010
2	Lehigh University Center for the Application of Mathematics ATTN: E. Varley R. Rivlin Bethlehem, PA 18015

No. Copies	Organization
1	North Carolina State University Dept. of Civil Engineering ATTN: Y. Horie Raleigh, NC 27607
1	Rice University Dept. of Mathematical Sciences ATTN: C.-C. Wang PO Box 1892 Houston, TX 77001
3	The Johns Hopkins University Dept. of Mechanical Engineering Latrobe Hall ATTN: W. Sharp R. Green A. Douglas 34th and Charles Streets Baltimore, MD 21218
1	Tulane University Dept. of Mechanical Engineering ATTN: S. Cowin New Orleans, LA 70112
1	University of California at Santa Barbara Dept. of Materials Science ATTN: A. Evans Santa Barbara, CA 93106

DISTRIBUTION LIST

No. Copies	Organization
5	University of California at San Diego Dept. of Applied Mechanics and Engineering Sciences ATTN: S. Nemat-Nasser M. Meyers G. Ravichandran X. Markenscoff A. Hoger La Jolla, CA 92093
1	Northwestern University Dept. of Applied Mathematics ATTN: W. Olmstead Evanston, IL 60201
4	University of Florida Dept. of Engineering Science and Mechanics ATTN: L. Malvern D. Drucker E. Walsh M. Eisenberg Gainesville, FL 32601
2	University of Houston Dept. of Mechanical Engineering ATTN: L. Wheeler R. Nachlinger Houston, TX 77004

No. Copies	Organization
2	University of Illinois Dept. of Theoretical and Applied Mechanics ATTN: D. Carlson D. Stewart Urbana, IL 61801
2	University of Illinois at Chicago Circle Dept. of Engineering, Mechanics, and Metallurgy ATTN: T. Ting D. Krajcinovic PO Box 4348 Chicago, IL 60680
2	University of Kentucky Dept. of Engineering Mechanics ATTN: M. Beatty O. Dillon, Jr. Lexington, KY 40506
1	University of Kentucky School of Engineering ATTN: R. Bowen Lexington, KY 40506
2	University of Maryland Dept. of Mathematics ATTN: S. Antman T. Liu College Park, MD 20742

DISTRIBUTION LIST

No. Copies	*Organization*
3	University of Minnesota Department of Aerospace Engineering and Mechanics ATTN: J. Erickson R. Fosdick R. James 110 Union Street SE Minneapolis, MN 55455
2	University of Oklahoma School of Aerospace, Mechanical, and Nuclear Engineering ATTN: A. Khan C. Bert Norman, OK 73019
4	University of Texas Dept. of Engineering Mechanics ATTN: M. Stern M. Bedford J. Oden Austin, TX 78712
1	University of Washington Dept. of Aeronautics and Astronautics ATTN: I. Fife 206 Guggenheim Hall Seattle, WA 98195
2	University of Maryland Dept. of Mechanical Engineering ATTN: R. Armstrong J. Dally College Park, MD 20742

No. Copies	*Organization*
1	University of Wyoming Dept. of Mathematics ATTN: R. Ewing PO Box 3036 University Station Laramie, WY 82070
3	Washington State University Dept. of Physics ATTN: R. Fowles G. Duvall Y. Gupta Pullman, WA 99163
1	Yale University Dept. of Mechanical Engineering ATTN: E. Onat 400 Temple Street New Haven, CT 96520
1	Institute for Defense Analysis ATTN: G. Mayer 1801 N. Beauregard Street Alexandria, VA 22311
1	Honeywell, Inc. Defense Systems Division ATTN: G. Johnson 600 Second Street NE Hopkins, MN 55343

DISTRIBUTION LIST

No. Copies	*Organization*
7	SRI International ATTN: D. Curran R. Shockey L. Seaman D. Erlich A. Florence R. Caliguri H. Giovanola 333 Ravenswood Avenue Menlo Park, CA 94025
1	Southwest Research Institute Department of Mechanical Sciences ATTN: U. Lindholm 8500 Culebra Road San Antonio, TX 02912
	Aberdeen Proving Ground
	Dir, USAMSAA ATTN: AMXSY-D AMXSY-MP/H. Cohen
	Cdr, USATECOM ATTN: AMSTE-TO-F
	Cdr, CRDEC, AMCCOM ATTN: SMCCR-RSP-A SMCCR-MU SMCCR-SPS-IL

DISTRIBUTION LIST

No. Copies	Organization
1	Commander US Army Research and Standardization Group (Europe) ATTN: F. Oertel P. O. Box 65 FPO, NY 09510

USER EVALUATION SHEET/CHANGE OF ADDRESS

This laboratory undertakes a continuing effort to improve the quality of the reports it publishes. Your comments/answers below will aid us in our efforts.

1. Does this report satisfy a need? (Comment on purpose, related project, or other area of interest for which the report will be used.) ____________________

2. How, specifically, is the report being used? (Information source, design data, procedure, source of ideas, etc.) ____________________

3. Has the information in this report led to any quantitative savings as far as man-hours or dollars saved, operating costs avoided, or efficiencies achieved, etc? If so, please elaborate. ____________________

4. General Comments. What do you think should be changed to improve future reports? (Indicate changes to organization, technical content, format, etc.) ____________________

BRL Report Number ____________ Division Symbol ____________

Check here if desire to be removed from distribution list. ____

Check here for address change. ____

Current address: Organization ____________________
Address ____________________

-------------------------------FOLD AND TAPE CLOSED---------------------------

Director
U.S. Army Ballistic Research Laboratory
ATTN: SLCBR-DD-T(NEI)
Aberdeen Proving Ground, MD 21005-5066

OFFICIAL BUSINESS
PENALTY FOR PRIVATE USE $300

NO POSTAGE NECESSARY IF MAILED IN THE UNITED STATES

BUSINESS REPLY LABEL
FIRST CLASS PERMIT NO. 12062 WASHINGTON D.C.

POSTAGE WILL BE PAID BY DEPARTMENT OF THE ARMY

Director
U.S. Army Ballistic Research Laboratory
ATTN: SLCBR-DD-T(NEI)
Aberdeen Proving Ground, MD 21005-9989